EFFECT OF ELEVATED TEMPERATURES ON THE BOND BEHAVIOUR OF GFRP BARS TO CONCRETE – PULL-OUT TESTS

Luís Miguel Rosado Granadeiro

Keywords: GFRP rebars; GFRP-concrete bond; elevated temperature; pull-out tests; bond-slip models.

Abstract. *Glass fibre reinforced polymer (GFRP) rebars are being increasingly used to reinforce either new or existing (degraded) concrete structures, owing to the advantages they offer over steel reinforcement, such as lightness and especially corrosion resistance. However, the strength, stiffness and bond properties of these materials are severely deteriorated at moderately elevated temperatures, namely when approaching the glass transition temperature (T_g) of the polymer matrix, which is typically in the range of 65-150 ºC. The first part of this paper presents an experimental investigation on the bond between concrete and sand coated GFRP rebars at moderately elevated temperatures. Pull-out tests were performed on GFRP rebars embedded in concrete cylinders at 20 ºC, 60 ºC, 100 ºC and 140 ºC; two bond lengths of the GFRP rebars were considered, corresponding to 5 and 9 times their diameter. Specimens were first heated up to the predefined temperature (measured at the GFRP-concrete interface) and then loaded up to failure. The applied load and the slip of the rebars at both their loaded and free ends were measured during the tests. The results obtained confirmed that the stiffness and strength of the GFRP-concrete interface suffers significant reductions with temperature, especially when the T_g of the GFRP rebars is approached and exceeded. In the second part of the paper, a bond vs. slip relation for the GFRP-concrete interface is proposed for each of the tested temperatures; this relation was derived based on a fitting procedure of the experimental data to a bond vs. slip model available in the literature for FRP bars in concrete, originally developed for ambient temperature. Additionally, the accuracy of two empirical (relaxation) models, proposed by Gibson et al. and Correia et al. in predicting the GFRP-concrete bond strength reduction with temperature was also assessed.*

1 INTRODUCTION

Glass fibre reinforced polymer (GFRP) rebars have been emerging has a non-corrodible alterative to ordinary steel reinforcement, especially in highly corrosive environments where the durability of constructions is an issue. GFRP rebars present other advantages, such as low weight, high tensile strength and electromagnetic transparency, making them suitable for applications in both new construction and rehabilitation of existing degraded reinforced concrete (RC) structures (*e.g.*, as a replacement for steel-corroded rebars) [1].

In spite of such potential, there are serious concerns about the behaviour of GFRP rebars at elevated temperature and under fire exposure, since their mechanical properties (namely, the tensile strength and the E-modulus) experience significant reductions, especially when approaching the glass transition temperature (T_g) of the polymeric matrix (usually between 65-150 ºC [2]). Despite its relevance, the fire performance of GFRP materials and GFRP-RC structures is still not well understood in the literature, which explains why a great majority of existing design guidelines do not recommend the use of GFRP rebars in structures where the fire action has to be considered at design (*i.e.*, in buildings) [1].

Moreover, elevated temperature has been referred to play an important role on the deterioration of the bond capacity of GFRP rebars in concrete [3]. This is particularly worrying, even for moderately elevated temperatures, since several authors (*e.g.*, [4, 5]) have reported premature structural collapses of GFRP-RC slabs exposed to fire, due to the rebar's debonding in the lap-slices. Despite its importance, few studies have been developed about this topic.

Katz *et al.* [3] performed pull-out tests in steel and GFRP rebars with different superficial finishes. The T_g of the GFRP rebars ranged from 60 ºC to 124 ºC. The steel/GFRP-concrete specimens, with an embedment length in concrete of 5 diameters, were heated up from room temperature (20 ºC) up to 250-350 ºC (measured at the centre of the specimens). The following conclusions were obtained: (i) for GFRP bars most part of the bond strength reduction occurred for temperatures below 180-200 ºC; (ii) at 200 ºC, the GFRP bond strength was reduced at least 80% (compared to that measured at room temperature), while in the steel rebars the bond losses, at that temperature, were only of 38%; (iii) above 200 ºC, the bond strength did not exhibit significant further reductions with temperature.

Further studies conducted by Katz and Berman [6] validated the results obtained in the previous study, and allowed concluding that the bond strength depends firstly and mostly on parameters associated with the surface properties and geometry of the rebars. The authors identified the following parameters as being the most relevant to the GFRP-concrete bond degradation with temperature: (i) the bond strength at room temperature (provided by the surface finishing and roughness of the reinforcement); (ii) the glass transition temperature of the material at the surface of the rebar; (iii) the residual bond strength, *i.e.*, at temperatures below 350 ºC, where no further reduction of the bond strength occurred; (iv) the degree of crosslinking (as the number of crosslinks increase, the nature of the polymer is expected to change, from thermoplastic to thermosetting, allowing to slow down the degradation rate of the material as temperature increases).

Bisby *et al.* [7] studied the GFRP-concrete bond performance, from temperatures that varied roughly between 25 ºC and 150 ºC, of GFRP rebars with two types of surface finishing: (i) a thin sand coating associated with a double helical fibre wrap (BPG rebar); and (ii) a coarse sand coating (PTG rebar). The glass transition temperatures of the rebars were 86 ºC and 84 ºC, respectively (based on the onset of the storage modulus curve). The embedment length of the rebars in concrete was approximately 4 times the diameter of the rebars. A steep reduction of the bond strength occurred below the glass transition temperature of the rebars: at that temperature, strength retentions were about 54 and 44% (compared to the bond strength at 25 ºC), for the BPG and PTG rebars, respectively. At 150 ºC, bond strength retentions were 37% for the BPG rebar and only 18% for the PTG rebar. However, it should be noted that the vast majority of the specimens exhibited splitting failure, instead of the desired pull-out failure.

In light of the brief literature review presented above, a set of aspects arise as issues of great importance. Firstly, the number of existing studies about the reduction of the GFRP bond properties with temperature is very limited. Therefore, additional and more comprehensive investigations are required to fully understand the degradation mechanisms that take place at the GFRP-concrete interface, and their influence on the structural performance of GFRP-RC structures exposed to elevated temperature and fire conditions. Secondly, additional experimental studies are needed to further evaluate the temperature dependence of a set of parameters, expected to affect the bond properties of the rebars at elevated temperature, namely: surface finishing, diameter, geometry and embedment length in concrete. Finally, bond-slip models that describe the GFRP-concrete bond constitutive relation as a function of temperature are also not available in the literature.

This paper presents experimental and analytical investigations on the effects of moderately elevated temperatures on the bond between GFRP rebars and concrete. In this regard, pull-out tests were performed in sand coated GFRP rebars, embedded in concrete cylinders, from room temperature up to 140 ºC. The influence of two different bond lengths (5 and 9 times the diameter of the rebars) in the bond properties at elevated temperature was investigated. The analytical studies presented in the second part of this paper aimed at: (i) proposing a temperature-dependent bond stress-slip model (based on the BPE Modified Model, originally proposed for room temperature [8]), and (ii) evaluating the accuracy of two empirical models, described in the literature, in modelling the effect of temperature on the bond strength.

2 EXPERIMENTAL PROGRAMME

2.1 Test programme

The experimental campaign comprised pull-out tests on sand coated GFRP rebars, embedded in concrete cylinders, at the following four temperatures: 20 ºC, 60 ºC, 100 ºC and 140 ºC. Two series of pull-out tests were carried out, corresponding to two different embedment lengths (L_b) of the GFRP rebars in concrete: 5 and 9 times the diameter (d_b) of the rebars - 50 and 90 mm, respectively.

2.2 Materials

Sand coated GFRP rebars with a vinylester matrix and external helically wound fibres were used in this study. The rebars were 10 mm in diameter and were supplied by *Hughes Brothers* (model *Aslan 100*). Dynamic mechanical analyses (DMA) were performed as defined in [9] and allowed defining a glass transition temperature of 98 ºC based on the onset of the storage modulus curve (average value between three curves) (Figure 1).

Previous tensile tests at elevated temperatures (from room temperature up to 300 ºC) on these rebars were performed by Santos [10] according to the standards [11, 12]. The results (Figure 2) showed that the tensile strength decreased significantly when the glass transition temperature was reached, presenting average reductions of 40% and 43%, at 150 ºC and 300 ºC, respectively, when compared to the strength at room temperature. The elasticity modulus was substantially less reduced at 300 ºC, exhibiting an average reduction of

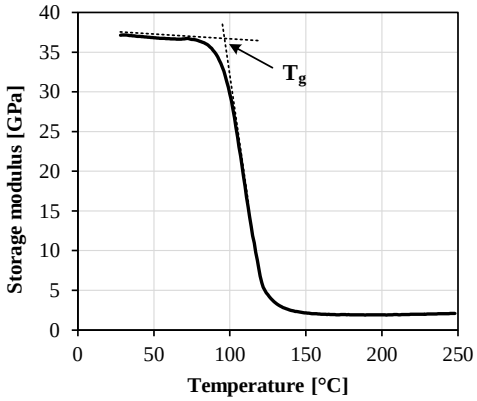

Figure 1: DMA results (storage modulus curve as a function of temperature).

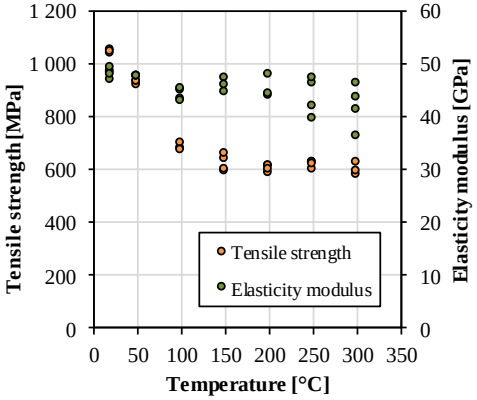

Figure 2: Tensile properties of GFRP rebars as a function of temperature.

13% compared to that measured at room temperature.

Concrete class C25/30 with cement type CEM II/A-L 42.5R and limestone aggregates was used to produce the specimens for the pull-out tests. The concrete's tensile and compressive properties were determined at the age of 111 days (age of testing). During that period, the test specimens, as well as the cylinders and cubes used to characterize the concrete's properties, were cured in the laboratory facilities at room temperature and relative humidity (indoor, but not controlled). The compressive and splitting tensile strength tests were performed according to standard procedures ([13] and [14], respectively), providing the following average values: cube compressive strength of 43.3 MPa and splitting tensile strength of 3.1 MPa.

2.3 Geometry of the specimens

The test specimens consisted of concrete cylinders (height of 150 mm, diameter of 150 mm) with a single GFRP rebar (length of 745 mm) embedded vertically along the central axis of the cylinder. The unbonded length of the rebars was set using a bond breaker made of a PVC tube, as shown in Figure 3. At the free end, the rebars were slightly protruded from the concrete cylinder, thus allowing to read the slip between that end of the rebar and the top surface of the concrete (with a video extensometer, as explained below). The loaded end of the rebars was protected using stainless steel tubes (diameter of 22 mm, 0.7 mm thick) to prevent premature tensile failure at the grip of the universal testing machine (*cf.* Figure 4).

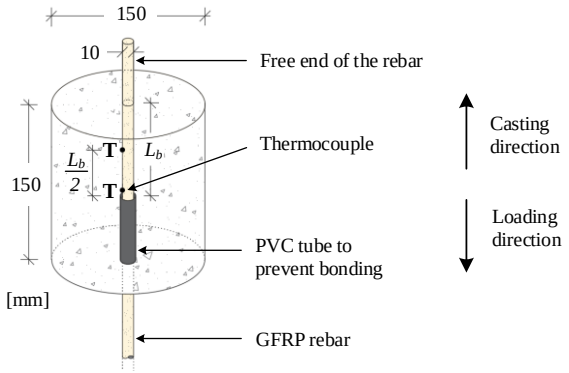

Figure 3: Pull-out test specimen geometry and thermocouples placement.

2.4 Test setup and instrumentation

The test setup used in the pull-out test is illustrated in Figure 4. The concrete specimens were placed on a metal frame composed by two metal plates, connected with steel rods, which acted as a reaction device. The

frame was installed inside a *Tinius Olsen* thermal chamber (Figure 4 b) and coupled to an *Instron* universal testing machine (load capacity of 250 kN).

The specimens' temperature was measured with 0.25 mm diameter type K thermocouples, positioned in the rebars as illustrated in Figure 3: at mid-height of the embedment length and in the transition between the bonded and unbonded lengths. An additional thermocouple was used to control the temperature inside the thermal chamber. The slip of the rebars was measured at both free and loaded ends using a video extensometer (Figure 4c); the equipment consists of a high definition video camera (*Sony*, model *XCG 5005E*, with *Fujinon* lens, model *Fujifilm HF50SA-1*), placed on a tripod. As Figure 4a illustrates, target dots were market on the GFRP rebar (free and loaded ends) and on angle brackets (fixed to the concrete's surface and to the bottom plate, respectively), allowing to measure the relative displacement (*i.e.*¸ the slip) between the rebar and the concrete.

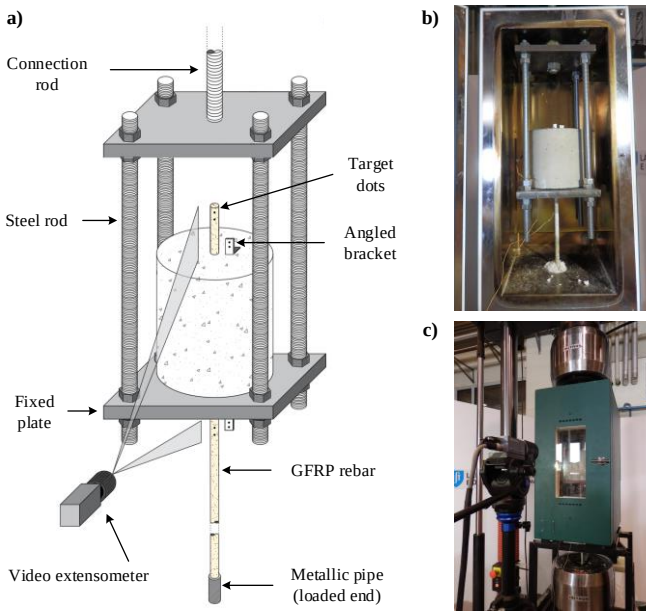

Figure 4: (a) Pull-out test setup; (b) general view of specimen in the thermal chamber; (c) external view of thermal chamber and video extensometer.

2.5 Test procedure

The experimental procedure consisted of two different stages; in the first stage of the test, the specimens were heated up to a predefined temperature, at an average heating rate of the air inside the thermal chamber of 8.4 ºC/min; the second stage, during which the specimens' temperature was kept constant at a specified value, consisted of loading the specimen (*i.e.*, pulling the GFRP rebar) until failure, under displacement control, at an approximate speed of 1 mm/min (test speed defined according to the limits set in ASTM D7913 [15]). During this stage, the applied load, the cross-head displacement of the test machine and the position of the target dots were monitored. The tests were carried out until the target dots were no longer traceable (by the video extensometer) or the maximum displacement of the testing machine was reached. For each temperature and bond length, at least three replicate specimens were tested.

3 EXPERIMENTAL RESULTS AND DISCUSSION

3.1. Load *vs.* cross-head displacement curves and load *vs.* slip curves

Figure 5 presents for each target temperature and bond length, the load-displacement curves of one representative specimen of each series. The displacement measurement corresponds to the cross-head displacement of the test machine, thus comprising: (i) the GFRP-concrete interface slip; (ii) the elongation of the rebar and the test setup components; and (iii) the possible slip in the grips. To simplify the analysis described in the present section, all curves are only plotted up to (a common) cross-head displacement of 25 mm.

Regardless of the bond length, the curves reflected an approximately linear behaviour until the maximum load was attained, which was followed by a sudden load drop (with exception of the specimens tested at 100 ºC, where such drop did not occur); this load drop was followed by a progressive load reduction (presenting almost a plateau for higher displacements). This final stage of the curves extended up to the end of the tests, which were interrupted

before the pull-out of the rebars (this issue will be further addressed in section 3.2). The specimens tested at 100 ºC presented a different post-peak behaviour compared to the remaining specimens: (i) after the maximum load was attained, the load presented a significantly less expressive drop; and (ii) in the specimens with bond lengths of $5d_b$, the maximum load was attained for considerably higher displacements. A possible explanation to this difference may be related to the fact that this temperature virtually matches the glass transition temperature of the rebars (98 ºC).

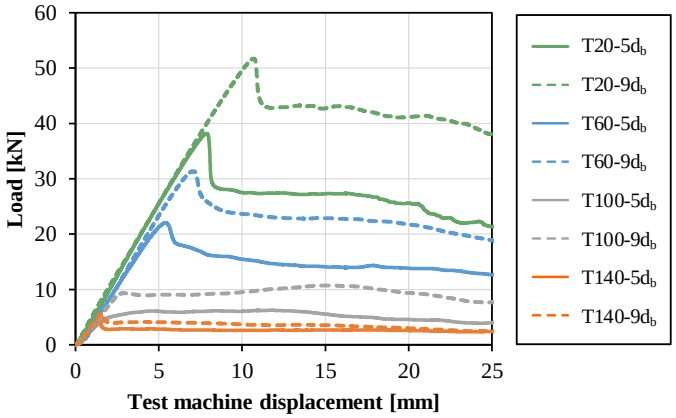

Figure 5: Load-displacement curves (cross-head displacement of the test machine) for representative specimens of all tested temperatures.

Figure 5 shows that: (i) for a certain temperature, as expected, the specimens with a longer bond length were able to attain higher loads; (ii) the maximum load was progressively reduced as the testing temperature increased. The effect of elevated temperature was also noticeable in the reduction of the global stiffness (corresponding to the slope of the initial linear branch); this result was expected, since for elevated temperatures the stiffness and strength of the constituent materials and especially of the GFRP-concrete interface are reduced.

Figure 6 and Figure 7 present the average bond stress *vs.* slip curves, corresponding to the loaded and free end slips, respectively, of one representative specimen of each series. Overall, the curves exhibited a similar behaviour to the load-displacement curves presented in Figure 5. However, the curves in Figure 7 (*i.e.*, the bond stress *vs.* free end slip curves) exhibited a slight stiffness increase from room temperature to 60 ºC. This may be explained by the fact that, at 60 ºC, the radial expansion of the rebar was more significant than the thermal degradation of the materials and of the GFRP-concrete interface. This may have increased the friction between the rebar and the concrete and, consequently, the interface stiffness.

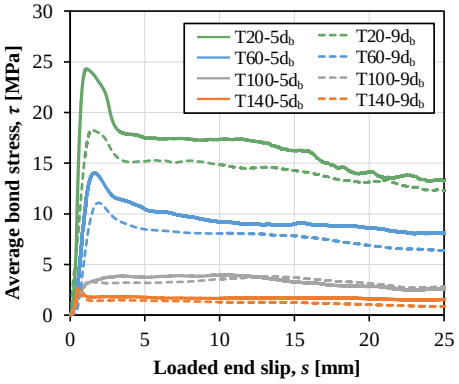

Figure 6: Average bond stress *vs.* loaded end slip curves for representative specimens of all tested temperatures.

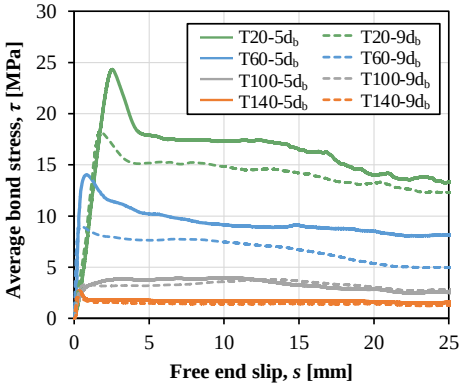

Figure 7: Average bond stress *vs.* free end slip curves for representative specimens of all tested temperatures.

3.2. Failure modes

The expected failure mode of the specimens consisted of pull-out of the GFRP rebars. Although the tests were interrupted before the complete pull-out of the rebars (because the video extensometer dots were no longer trackable or the stroke of the test machine was attained), no splitting failure was observed. The experimental

results (described in the previous section) and the visual observations of the specimens throughout the tests (*e.g.*, Figure 8a and b) validated the expected failure mode of the specimens by pull-out.

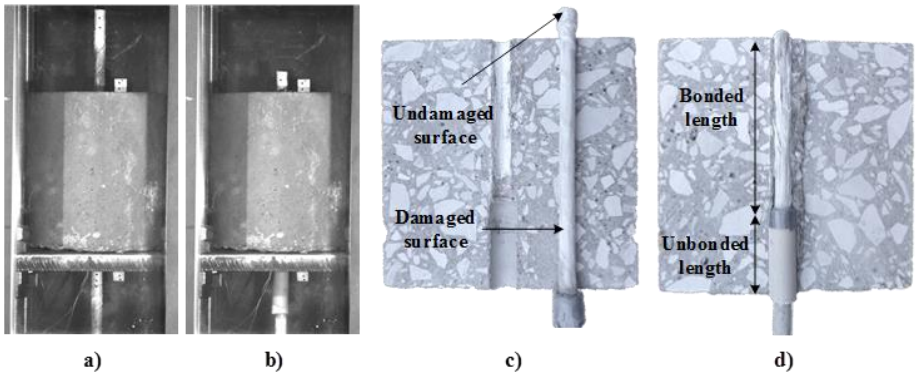

Figure 8: Slip of the rebar (free end) at the beginning (a) and end of the test (b); GFRP-concrete specimens tested at elevated temperature (c) and at room temperature (d).

After the tests, all concrete cylinders were saw cut into two pieces to confirm the failure modes and evaluate the damage underwent by the materials and the GFRP-interface. As shown in Figure 8c, the external layer of the GFRP rebars was significantly abraded; in particular, the wound fibres were ripped and the sand-coated superficial layer was peeled; residues of crushed resin and broken glass fibres were attached to the concrete (along the embedment length of the rebar). No damage on the core of the rebar was observed. However, in some specimens tested at room temperature (Figure 8d), the abrasion introduced to the rebar was more severe: the superficial layer of sand and the wound fibres were completely removed, the core of the rebar was exposed, and a substantial amount of longitudinal fibres were broken and stripped from the core.

A possible explanation for the plateau of the load-displacement curves plotted in Figure 5 (presented in section 3.1) is the entrance of the free end length of the rebar into the concrete cylinder. When in contact with the concrete's surface, this undamaged portion of the rebar provided an increase in the GFRP-concrete friction, compared to the one provided by the damaged (and initially embedded) length of the rebar, thus providing an additional contribution to the overall resistance against slip.

3.3. Bond strength

Figure 9 presents the variation of the normalized average bond strength with temperature. This figure shows that the bond strength was significantly reduced with temperature, even for temperatures well below the glass transition temperature of the GFRP rebars. As shown in Table 1, for a temperature as low as 60 ºC (that can be attained in outdoor applications), bond strength retentions were about 60% of that at room temperature (20 ºC), while for 100 ºC and 140 ºC retentions were only of 20% and 10%, respectively. Moreover, the results highlighted that: (i) the bond strength exhibited a similar decrease with temperature for the two test series (*i.e.*, for the two different bond lengths); (ii) the reduction of the GFRP-concrete bond strength occurred for lower temperatures than the mechanical degradation at the material level (as measured in the tensile tests and in the DMA tests, *cf.* Figure 9).

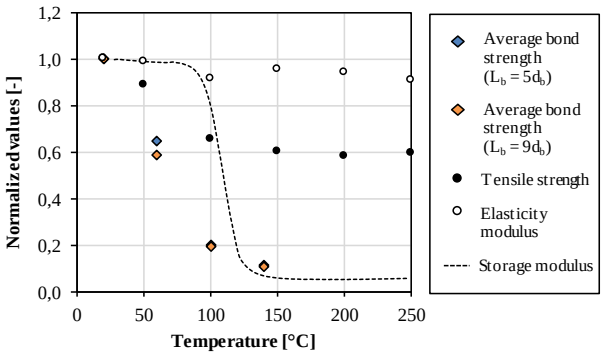

Figure 9: Normalized average values of bond strength, tensile strength, elasticity and storage modulus, as a function of temperature.

Table 1: Results obtained in terms of maximum load, bond stress and normalized maximum load (average ± standard deviation).

Temperature [ºC]	**Bond length to concrete = $5d_b$**			**Bond length to concrete = $9d_b$**		
	Maximum load [kN]	Bond stress [MPa]	Normalized maximum load [-]	Maximum load [kN]	Bond stress [MPa]	Normalized maximum load [-]
20 ± 2	35.7 ± 4.4	22.7 ± 2.8	1.00	52.6 ± 3.8	18.6 ± 1.4	1.00
60 ± 2	23.0 ± 1.7	14.6 ± 1.1	0.64	30.8 ± 5.1	10.9 ± 1.8	0.58
100 ± 2	7.2 ± 1.6	4.6 ± 1.0	0.20	10.1 ± 3.4	3.6 ± 1.2	0.19
140 ± 2	3.9 ± 0.3	2.5 ± 0.2	0.11	5.5 ± 0.5	1.9 ± 0.2	0.10

4 ANALYTICAL STUDY

4.1 Bond vs. slip curves

The bond behaviour between reinforcing bars and concrete is usually described through bond stress *vs.* slip relations/models; however, for GFRP rebars there is still no unified model to reproduce their bond behaviour to concrete. A recent state of the art review [16] about this topic summarized the bond models that have been used in the literature for GFRP rebars; additionally, the accuracy of these bond models in reproducing GFRP-concrete bond at ambient temperature was also assessed; it was concluded that a modified version of the BPE model (originally developed for steel rebars) proposed by Cosenza *et al.* [8] (*cf.* Figure 10a) is able to accurately simulate the GFRP-concrete bond, provided that its defining parameters are properly fitted to experimental data. This model is characterized by three stages (*cf.* Figure 10a): (i) a nonlinear ascending stage (equation 1); (ii) a linear descending branch (equation 2); and (iii) a final plateau.

In the present paper, a slightly different version of the BPE modified model is proposed, in which the final plateau is replaced by an additional descending branch (equation 3), in agreement with the behaviour observed in the experimental data (*cf.* Figure 6). The parameters involved in equations (1) to (3) were obtained for all tested temperatures and both bond lengths based on a fitting procedure that minimizes the mean square error to the experimental bond *vs.* slip curves.

$$\tau(s) = \tau_{max}\left(\frac{s}{s_1}\right)^{\alpha} \tag{1}$$

$$\tau(s) = \tau_{max} - \tau_{max}\, p_1\left(\frac{s}{s_1} - 1\right) \tag{2}$$

$$\tau(s) = \tau_f - \tau_f\, p_2\left(\frac{s}{s_2} - 1\right) \tag{3}$$

Table 2 lists the parameters obtained for the different temperatures and bond lengths and Figure 10b plots the corresponding bond *vs.* slip curves. As expected, the curves present a similar overall behaviour when compared to the experimental ones (*cf.* Figure 6); this good agreement is attested by the relatively low values of the absolute mean percentage error (AMPE). It is worth mentioning that the bond *vs.* slip curves proposed herein are valid for the specific GFRP rebars used in the tests; the adequacy of these bond models for different GFRP rebars (and surface finishing) at the different temperatures needs to be further investigated.

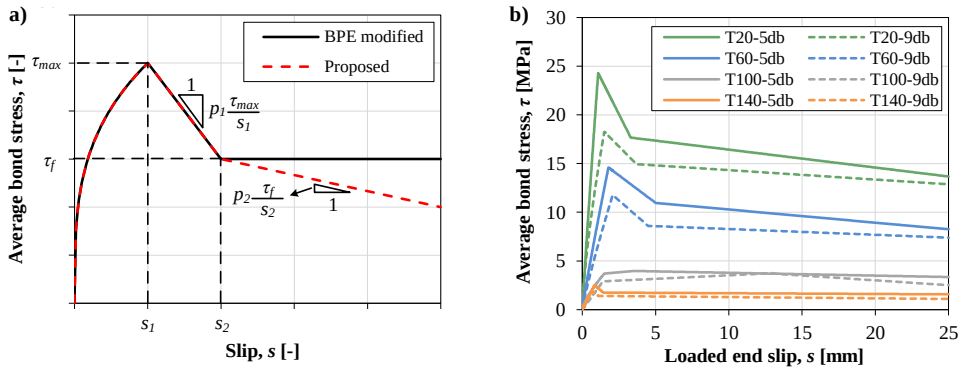

Figure 10: a) BPE modified model and proposed model; b) calibrated bond *vs.* slip relations.

Table 2: Parameters of the calibrated bond *vs.* slip relations (see equations (1) to (3)) for all tested temperatures and both bond lengths; absolute mean percentage errors (AMPE).

Temperature	20 ºC		60 ºC		100 ºC		140 ºC	
Bond length	$5d_b$	$9d_b$	$5d_b$	$9d_b$	$5d_b$	$9d_b$	$5d_b$	$9d_b$
τ_{max} [MPa]	24.3	18.3	14.6	11.8	3.7	2.9	2.5	1.9
s_1 [mm]	1.08	1.50	1.78	2.07	1.50	1.40	0.83	0.63
α [-]	0.940	0.717	0.920	0.875	0.728	1.010	1.081	0.794
p_1 [-]	0.133	0.125	0.138	0.230	-0.055	-0.035	0.420	0.350
τ_f [MPa]	17.7	14.9	11.0	8.6	4.0	3.7	1.8	1.4
p_2 [-]	0.034	0.024	0.062	0.031	0.026	0.349	0.006	0.010
s_2 [mm]	3.30	3.69	5.00	4.51	3.5	13.00	1.44	1.10
AMPE [%]	13.3	9.9	10.1	11.1	13.8	10.2	5.8	10.7

4.2 Degradation models

In addition to the bond *vs.* slip curves presented in the previous section, the ability of the empirical models proposed by Gibson *et al.* [17] and Correia *et al.* [18] in simulating the variation of the average bond strength with temperature was assessed. These relaxation models involve curve fitting procedures to the experimental results and have been successfully used to simulate the mechanical properties of FRP materials at elevated temperatures [18].

According to Gibson *et al.* [17], the variation of a generic mechanical property (*P*) with temperature (*T*) can be defined by the following equation,

$$P(T) = P_u - \frac{P_u - P_r}{2} \times (1 + \tanh[k'(T - T_{g,mech})]) \quad (4)$$

where P_u is the value of the property at room temperature and P_r is the value of the property after the glass transition (but before decomposition). The parameters k' and $T_{g,mech}$ are obtained by fitting the theoretical curve to the experimental data.

Correia *et al.* [18] proposed the following model, which is based on the Gompertz statistical distribution,

$$P(T) = P_r + (P_u - P_r) \times (1 - e^{Be^{C \times T}}) \quad (5)$$

where the parameters B and C are fitted to the experimental data.

Since the bond strength obtained for both bond lengths presented a similar reduction with temperature, the equations described above were simultaneously fitted to the experimental data of both bond lengths using a standard procedure that minimizes the mean square errors.

Figure 11 plots the theoretical curves of the models used, together with the normalized experimental values of the average bond strength. It can be seen that both models present a good agreement with the experimental results (slightly better for Gibson *et al.*'s model), *i.e.* they are able to provide accurate estimates of the GFRP-concrete bond strength reduction with temperature. Table 3 lists the parameters obtained for the two models and the respective absolute mean percentage errors (AMPE).

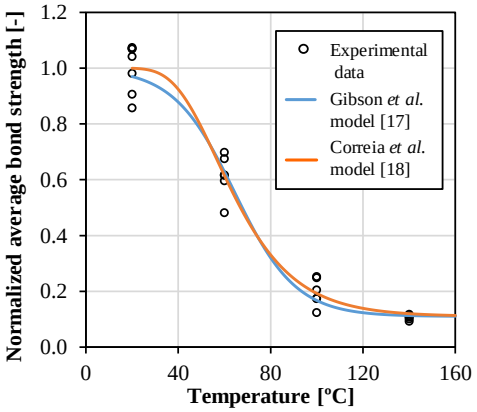

Figure 11: Normalized average bond strength (compared to room temperature) *vs*. temperature: experimental results and modelling curves.

Table 3: Simulation of the bond strength degradation with temperature – defining parameters and absolute mean percentage error (AMPE).

Model	**Parameter**	
Gibson *et al.* [17]	P_u [-]	1.00
	P_r [-]	0.11
	k' [-]	0.0377
	$T_{g,mech}$ [ºC]	64.41
	AMPE [%]	11.5
Correia *et al.* [18]	B [-]	-21.20
	C [-]	-0.05
	AMPE (%)	12.4

5 CONCLUSIONS

This paper presented experimental and analytical investigations about the bond behaviour between GFRP rebars (sand coated with external helically wound fibres) and concrete from room temperature up to 140 ºC. From the results obtained, the following main conclusions can be drawn:

1. As expected, the strength and stiffness of the GFRP-concrete interface are significantly affected with increasing temperatures. The average bond strength is severely reduced at elevated temperature, for temperatures well below the glass transition temperature of the GFRP rebars (98 ºC), presenting retentions of 60% and of only 10% at respectively 60 ºC and 140 ºC, compared to the bond strength at room temperature.
2. For the materials, test setup and procedure, and range of temperatures tested, similar bond strength reductions with temperature were obtained for both bond lengths (5 and 9 times the diameter of the rebars).
3. Visual observations of the specimens after the tests allowed concluding that the damage undergone by the GFRP rebars was limited mostly to their surface, with the superficial layer of sand being completely stripped from the rebars' core.
4. An alternative version of the BPE modified model was proposed to describe the bond behaviour of the GFRP bars to concrete at different temperatures; this model presented a good agreement with the bond *vs.* slip curves experimentally obtained.
5. The empirical models assessed in the present study, proposed by Gibson *et al*. [17] and Correia *et al*. [18], were both able to accurately simulate the GFRP-concrete bond strength reduction with temperature.

ACKNOWLEDGMENTS

The author wishes to acknowledge FCT (project PTDC/ECM-EST/1882/2014) and CERIS for funding the research, Secil and Unibetão for supplying the concrete and Hughes Brothers for supplying the GFRP rebars.

REFERENCES

[1] Bank L.C., 'Composites for Construction - Structural Design with FRP Materials', Wiley, New Jersey, 2007.

[2] Mouritz A.P. and Gibson A.G., 'Fire Properties of Polymer Composite Materials', Springer, Dordrecht, 2006.

[3] Katz A., Berman N. and Bank L.C., 'Effect of high temperature on bond strength of FRP rebars', *ASCE Journal of Composites for Construction*, 3 (4), 153–160, 1999.

[4] Weber A., 'Fire-resistance tests on composite rebars', *Fourth International Conference of FRP Composites in Civil Engineering (CICE 2008)*, Zurich, Switzerland, (22-24/07), 2008.

[5] Abbasi A. and Hogg P.J., 'Fire testing of concrete beams with fibre reinforced plastic rebar', *Composites*

Part A: Applied Science and Manufacturing, 37 (8), 1142–1150, 2006.

[6] Katz A. and Berman N., 'Modeling the effect of high temperature on the bond of FRP reinforcing bars to concrete', *Cement & Concrete Composites*, 22 (6), 433–443, 2000.

[7] McIntyre E., Bisby L. and Stratford T., 'Bond strength of FRP reinforcement in concrete at elevated temperature', *Proceedings of the 7th International Conference on FRP Composites in Civil Engineering (CICE 2014)*, Vancouver, Canada, (20-22/08), 2014.

[8] Cosenza E., Manfredi G. and Realfonzo R., 'Behavior and Modeling of Bond of FRP Rebars to Concrete', *Journal of Composites for Construction*, 1 (2), 40–51, 1997.

[9] ASTM E1640, 'Standard Test Method for Assignment of the Glass Transition Temperature By Dynamic Mechanical Analysis', *American Society for Testing and Materials*, West Conshohocken, USA, 1999.

[10] Santos P., 'Fire Behaviour of GFRP Reinforced Concrete Slabs' (in Portuguese), *MSc dissertation in Civil Engineering*, Instituto Superior Técnico, Lisboa, Portugal, 2016.

[11] JSCE-E 531-1995, 'Test Method for Tensile Properties of Continuous Fiber Reinforcing Materials', *Japan Society of Civil Engineers*, Tokyo, Japan, 1995.

[12] ISO 10406-1, 'Fibre-reinforced polymer (FRP) reinforcement of concrete - Test methods - Part 1: FRP bars and grids', *Internation Standards Organization*, Geneva, Switzerland, 2008.

[13] CEN, 'Testing hardened concrete - Part 3: Compressive strength of test specimens', EN 12390-3, *European Committee for Standardization*, Brussels, Belgium, 2009.

[14] CEN, 'Testing hardened concrete - Part 3: Tensile splitting strength of test specimens', EN 12390-6, *European Committee for Standardization*, Brussels, Belgium, 2009.

[15] ASTM D7913/D7913M, 'Standard Test Method for Bond Strength of Fiber-Reinforced Polymer Matrix Composite Bars to Concrete by Pullout Testing', *American Society for Testing and Materials*, West Conshohocken, USA, 2014.

[16] Yan F., Lin Z. and Yang M., 'Bond mechanism and bond strength of GFRP bars to concrete: A review', *Composites Part B*, 98, 56–69, 2016.

[17] Gibson A.G., Wu Y.-S., Evans J.T. and Mouritz A.P., 'Laminate theory analysis of composites under load in fire', *Journal of Composite Materials*, 40 (7), 639–658, 2006.

[18] Correia J.R., Gomes M.M., Pires J.M. and Branco F.A., 'Mechanical behaviour of pultruded glass fibre reinforced polymer composites at elevated temperature: Experiments and model assessment', *Composite Structures*, 98, 303–313, 2013.